

TSF-1018

Numerical Study of Natural Convection Conjugating with Surface Radiation in a Square Enclosure: Effects of the Different Schemes Used to Discretize the Convective and Diffusive Terms of the Transport Equations

Uthai Prasopchingchana*, Kittipong Boonlong and Montana Rungsiyopas

Department of Mechanical Engineering, Faculty of Engineering, Burapha University, Chonburi 20131 Thailand

*E-mail: uthai@buu.ac.th, Tel.: (+66) 3810-2222, Fax.: (+66) 3874-5806

Abstract

This paper aims to investigate natural convection conjugating with surface radiation in a square enclosure. Convective and diffusive parameters of the transportation equations are calculated using discretized numerical method in the three schemes: central, upwind, and hybrid differencing schemes. In this work, the running time and the iteration number of computing in the various schemes are compared. As the vertical walls of the enclosure are differentially heated while the others are adiabatic, the analyses are performed in two dimensions and steady-state conditions. Air contained in the enclosure is treated as a compressible Newtonian fluid. An in-house code is developed for these cases providing numerical solutions which are compared with the results from the benchmark and the published correlation in order to validate the code. The relationship between the running time including the iteration numbers and Rayleigh numbers in the square enclosure with the various schemes and the surface emissivity are demonstrated. The results illustrate that the upwind differencing scheme can converge into the solutions slightly faster than the others for the surface emissivity of 0 and 1 but there is no significant in the varying schemes for the surface emissivity of 0.5.

Keywords: finite volume method, central differencing scheme, upwind differencing scheme, hybrid differencing scheme, natural convection, surface radiation.

1. Introduction

Natural convection and surface radiation is the important heat transfer modes occurring in many engineering applications such as heat transfer in nuclear reactors, heat transfer in cavities of electronic equipment or heat transfer in rooms of buildings etc. There are a lot of researchers have devoted their time and budgets to investigate about the natural convection and

surface radiation phenomena. Most of them have performed simulation in a square enclosure and a preferable method employed to discretize the transport equations is the finite volume method. The basic schemes of the finite volume method which are used to discretize the convective and diffusive terms of the transport equations are the central, upwind and hybrid differencing schemes.

TSF-1018

De Vahl Davis [1] and Saitoh and co-worker [2] provided the benchmark numerical solutions for natural convection of air in a square cavity with differentially heated walls and the others were adiabatic. They adopted the finite difference method to discretize the partial differential equations of the airflow. Balaji and Venkateshan [3] presented the correlations for free convection and surface radiation in a square cavity. The finite volume method was employed to solve for convection. Akiyama and Chong [4] reported the solutions of the numerical analysis of natural convection with surface radiation in a square enclosure. They performed the simulation of the buoyant flow of air in the enclosure by using the finite difference method. Nilesh Agrawal et al. [5] carried out the numerical investigation to obtain a correlation for heat transfer during laminar natural convection in an enclosure containing the uniform mixture of air and hydrogen. The finite volume method was used and the first order upwind differencing scheme for convective terms and the second order central differencing scheme for diffusive term were employed to discretize the governing equations of the flow. The numerical simulation of free convection of a nanofluid in a square cavity with an inside heater was performed by Mostafa Mahmoodi [6]. He used the finite volume method and the second order central differencing scheme for the diffusive term and the hybrid differencing scheme for convective term. Xaman and colleagues [7] investigated natural convection combined with surface thermal radiation in a square cavity with a glass wall. The governing equations of the flow were solved by using the finite volume method. The convective and

diffusive terms of the transport equations were discretized by using the hybrid differencing scheme and the second order central differencing scheme, respectively.

From the review of the former literature, the various schemes were used to discretize the convective and diffusive terms of the transport equations but there are not the evaluation of the convergent performance of the basic schemes. Therefore, the objectives of this work are aimed to investigate the performance of the developed code under the basic schemes of the finite volume method on the application of natural convection conjugating with surface radiation in a square enclosure. In addition, the investigation is carried out with air contained in the square enclosure and treated as a compressible Newtonian fluid.

2. Problem Statement and Mathematical

Model

The geometry of the problem under consideration is shown in Fig. 1. The square enclosure has the width and height of b , the characteristic length. The vertical hot and cold temperature sides are designated by T_H and T_C , respectively. The other sides are the adiabatic walls. The square enclosure is contained with air a nonparticipating media and the enclosure wall surfaces are assumed to be the diffuse gray surfaces.

TSF-1018

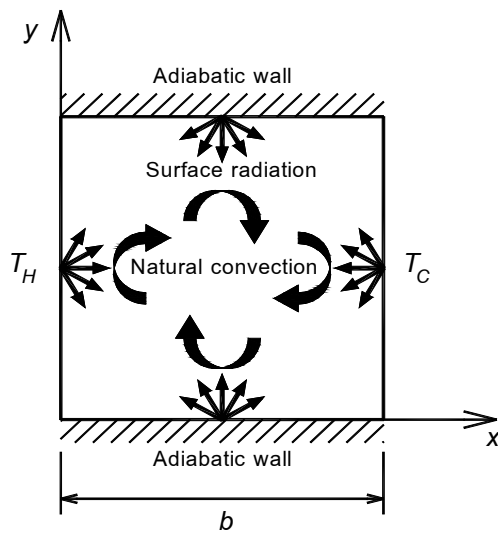


Fig. 1 Geometry of the problem.

2.1 Natural convection

Because of the temperature difference between the vertical hot and cold walls of the square enclosure, air circulation and natural convection occurs within the square enclosure. The governing equations of the airflow in the square enclosure are defined by the continuity, momentum and energy equations. The equations at the steady-state condition for a compressible Newtonian fluid are expressed as the following [8]:

- The continuity equation

$$\nabla \cdot (\rho \mathbf{V}) = 0 \quad (1)$$

- The momentum equation in the horizontal direction

$$\nabla \cdot (\rho u \mathbf{V}) = -\frac{\partial P}{\partial x} + \nabla \cdot (\mu \nabla u) + S_{Mx} \quad (2)$$

where

$$S_{Mx} = \frac{\partial}{\partial x} \left(\mu \frac{\partial u}{\partial x} \right) + \frac{\partial}{\partial y} \left(\mu \frac{\partial v}{\partial x} \right) + \frac{\partial}{\partial x} \left(\left(-\frac{2}{3} \mu \right) \nabla \cdot \mathbf{V} \right)$$

- The momentum equation in the vertical direction

$$\nabla \cdot (\rho v \mathbf{V}) = -\frac{\partial P}{\partial y} + \nabla \cdot (\mu \nabla v) - \rho g + S_{My} \quad (3)$$

where

$$S_{My} = \frac{\partial}{\partial x} \left(\mu \frac{\partial u}{\partial y} \right) + \frac{\partial}{\partial y} \left(\mu \frac{\partial v}{\partial y} \right) + \frac{\partial}{\partial y} \left(\left(-\frac{2}{3} \mu \right) \nabla \cdot \mathbf{V} \right)$$

- The energy equation

$$\nabla \cdot (\rho i \mathbf{V}) = -P \nabla \cdot \mathbf{V} + \nabla \cdot (k \nabla T) + \Phi \quad (4)$$

where

$$\Phi = \mu \left\{ 2 \left[\left(\frac{\partial u}{\partial x} \right)^2 + \left(\frac{\partial v}{\partial y} \right)^2 \right] + \left(\frac{\partial u}{\partial y} + \frac{\partial v}{\partial x} \right)^2 \right\} + \left(-\frac{2}{3} \mu \right) (\nabla \cdot \mathbf{V})^2$$

The appropriate boundary conditions for the airflow in the square enclosure are:

- at $x = 0, 0 < y < b$

$$u = v = 0, T = T_H, \frac{\partial P}{\partial x} = 0$$

- at $x = b, 0 < y < b$

$$u = v = 0, T = T_C, \frac{\partial P}{\partial x} = 0$$

- at $0 \leq x \leq b, y = 0$

$$u = v = 0, T = T_B, \frac{\partial P}{\partial y} = -\rho g$$

- at $0 \leq x \leq b, y = b$

TSF-1018

$$u = v = 0, T = T_T, \frac{\partial P}{\partial y} = -\rho g$$

$$(q''_i)_{rad} = J_i - \sum_{j=1}^N F_{ij} J_j \quad (7)$$

All properties of air in the square enclosure are the functions of the temperature and pressure. The air properties are obtained from National Institute of Standards and Technology (NIST) Standard Reference Database 23, Version 9.0 by the two variables polynomial regression. The air properties are obtained from

$$\begin{aligned} \phi = & (a_{11} + a_{21}T + \dots + a_{m1}T^{m-1}) \\ & + (a_{12} + a_{22}T + \dots + a_{m2}T^{m-1})P \\ & + \dots + (a_{1n} + a_{2n}T + \dots + a_{mn}T^{m-1})P^{n-1} \end{aligned} \quad (5)$$

where ϕ are the air property variables of density, thermal conductivity, viscosity and specific internal energy, a_{mn} are coefficients of the variables, and T and P are the absolute temperature and pressure of air in the square enclosure, respectively. The coefficients of determination (R^2) of the air properties received from the two variables polynomial regression are greater than 0.99. For all air properties, m and n equal 6.

2.2. Surface radiation

The Hottel's crossed string method is employed to determine the view factors of the wall surfaces of the square enclosure which the wall surfaces are assumed to be infinitely long in the z direction. Firstly, the radiosity values on the wall surfaces of the square enclosure have to be determined by

$$J_i = \varepsilon_i \sigma T_i^4 + (1 - \varepsilon_i) \sum_{j=1}^N F_{ij} J_j \quad (6)$$

The radiative heat flux on the wall surfaces of the square enclosure is given by

Since the bottom and top wall surfaces of the square enclosure are adiabatic, the temperature distribution on the bottom and top wall surfaces of the square enclosure can be determined by the heat balance between natural convection and surface radiation. The heat balance on the bottom and top wall surfaces of the square enclosure are the following:

- at the bottom wall surface

$$k_A \frac{\partial T}{\partial y} = (q''_i)_{rad} \quad (8a)$$

- at the top wall surface

$$-k_A \frac{\partial T}{\partial y} = (q''_i)_{rad} \quad (8b)$$

2.3 Heat transfer

The total average Nusselt number of the square enclosure is calculated by

$$\overline{Nu}_{total} = \overline{Nu}_{conv} + \overline{Nu}_{rad} \quad (9)$$

The total average convective Nusselt number of the square enclosure is given by

$$\overline{Nu}_{conv} = \frac{1}{b} \int_0^b \frac{(q''_{conv}|_{x=0} + q''_{conv}|_{x=b})}{2q''_{ref}} dy \quad (10)$$

The convective heat flux is calculated by

$$q''_{conv} = -k_A \frac{\partial T}{\partial x} \quad (11)$$

The reference heat flux is expressed as

$$q''_{ref} = k_A \frac{(T_H - T_C)}{b} \quad (12)$$

The total average radiative Nusselt number of the square enclosure is written as

TSF-1018

$$\overline{Nu}_{rad} = \frac{1}{b} \int_0^b \frac{\left((q''_i)_{rad} \Big|_{x=0} + (q''_i)_{rad} \Big|_{x=b} \right)}{2q''_{ref}} dy \quad (13)$$

3. Numerical Method

The continuity, momentum and energy equations for the simulations of the airflow in the square enclosure are numerically solved according to their boundary conditions. The finite volume method is employed to discretize the equations of the airflow and the staggered grid is used. The Pressure Implicit with Splitting of Operators (PISO) algorithm is adopted to solve the velocity-pressure coupling problem of the airflow. The Tri-Diagonal Matrix Algorithm (TDMA) is used to solve the matrix systems of the variables.

Eqs. (2) and (3) can be written in a form called the transport equation:

$$\nabla \cdot (\rho \phi \mathbf{v}) = \nabla \cdot (\mu \nabla \phi) + S_\phi \quad (14)$$

where ϕ are the variables of the velocity components in the horizontal and vertical directions. The equation obtained from integration and discretization of the transport equation by the finite volume method can be expressed as

$$a_P \phi_P = a_E \phi_E + a_W \phi_W + a_N \phi_N + a_S \phi_S + B \quad (15)$$

where $B = \iint S_\phi dx dy$

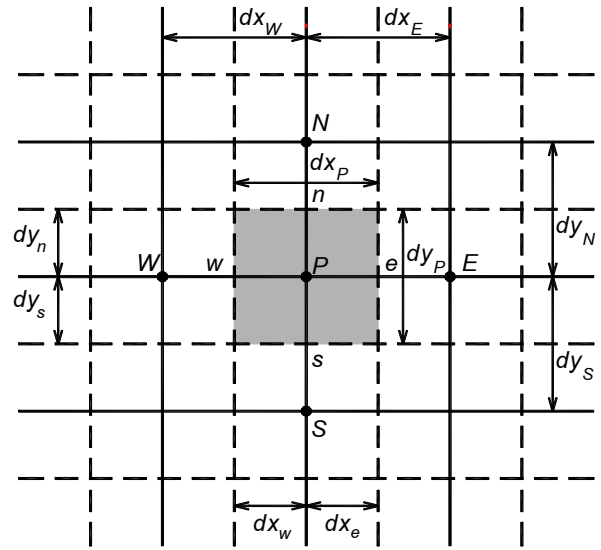


Fig. 2 Staggered grid.

3.1 Central differencing scheme

The coefficients of the neighbor variables of the discrete transport equation for the central differencing scheme are calculated by

$$a_E = DD_E - \frac{dx_e FF_E}{dx_E} \quad (16)$$

$$a_W = DD_W + \frac{dx_w FF_W}{dx_W} \quad (17)$$

$$a_N = DD_N - \frac{dy_n FF_N}{dy_N} \quad (18)$$

$$a_S = DD_S + \frac{dy_s FF_S}{dy_S} \quad (19)$$

3.2 Upwind differencing scheme

The coefficients of the neighbor variables of the discrete transport equation for the upwind differencing scheme are calculated by

$$a_E = DD_E + \text{MAX}[-FF_E, 0] \quad (20)$$

$$a_W = DD_W + \text{MAX}[FF_W, 0] \quad (21)$$

$$a_N = DD_N + \text{MAX}[-FF_N, 0] \quad (22)$$

TSF-1018

$$a_s = DD_s + \text{MAX}[FF_s, 0] \quad (23)$$

3.3 Hybrid differencing scheme

The coefficients of the neighbor variables of the discrete transport equation for the hybrid differencing scheme are calculated by

$$a_E = \text{MAX} \left[-FF_E, DD_E - \frac{dx_e FF_E}{dx_E}, 0 \right] \quad (24)$$

$$a_W = \text{MAX} \left[FF_W, DD_W + \frac{dx_w FF_W}{dx_W}, 0 \right] \quad (25)$$

$$a_N = \text{MAX} \left[-FF_N, DD_N - \frac{dy_n FF_N}{dy_N}, 0 \right] \quad (26)$$

$$a_S = \text{MAX} \left[FF_S, DD_S + \frac{dy_s FF_S}{dy_S}, 0 \right] \quad (27)$$

The coefficient of the property variable of the discrete transport equation for the all scheme is calculated by

$$a_P = a_E + a_W + a_N + a_S + (FF_E - FF_W + FF_N - FF_S) \quad (16)$$

where

$$DD_E = \frac{\mu_e dy_P}{dx_E}, \quad DD_W = \frac{\mu_w dy_P}{dx_W}$$

$$DD_N = \frac{\mu_n dx_P}{dy_N}, \quad DD_S = \frac{\mu_s dx_P}{dy_S}$$

$$FF_E = \rho_e u_e dy_P, \quad FF_W = \rho_w u_w dy_P$$

$$FF_N = \rho_n v_n dx_P, \quad FF_S = \rho_s v_s dx_P$$

For surface radiation, the radiosity values of the square enclosure wall surfaces are determined by the Gauss Seidel iteration method and the temperature distribution on the adiabatic wall surfaces of the square enclosure is

calculated by using heat balance between natural convection and surface radiation on the adiabatic wall surfaces of the square enclosure.

In the numerical procedures, the iteration processes have to be used to obtain the convergent solutions. Therefore, a convergent criterion is established to monitor the maximum relative difference of the velocities, temperatures and pressures in the two successive iterations. The maximum relative difference must be less than or equal to 10^{-4} , $\text{MAX} | (\phi^{\text{iter}} - \phi^{\text{iter-1}}) / \phi^{\text{iter}} | \leq 10^{-4}$, with $\phi = u, v, T, P$. A summary of the numerical procedures is:

1. The view factors of the wall surfaces of the square enclosure are calculated by the Hottel's crossed string method.
2. The initial guessed values for all of the variables are imposed.
3. The continuity and momentum equations of the airflow in the enclosure are solved under the PISO algorithm to obtain the velocity vectors and the pressure field by Eqs. (1) – (3).
4. The energy equations of the airflow in the square enclosure are solved to obtain the temperature distribution in the flow field by Eq. (4).
5. The radiosity and the surface radiation heat flux values of the wall surfaces of the square enclosure are determined by Eqs. (6) and (7), respectively. Then the temperature distribution on the

TSF-1018

adiabatic wall surfaces of the square enclosure is calculated by Eq. (8).

6. The convergent criterion is applied for all of the variables. If all of the variables do not meet the convergent criterion, The procedures must be returned to step 3, until the convergent criterion is achieved.

4. Code Validation

An in-house code is developed for this purpose. To insure that the solutions receiving from the developed code are correct, the validity of the code is demonstrated by comparing the solutions receiving from the code with the benchmark numerical solutions of De Vahl Davis [1], and Saitoh [2], the solutions from the published numerical correlations of Balaji [3] and the published numerical solution of Akiyama [4] in case there is only natural convection, and natural convection is conjugated with surface radiation.

Firstly, the grid independence test is conducted to insure that there is not the deviation of the solutions because of the grid sizes. The test is implemented in case natural convection is conjugated with surface radiation at $Ra = 10^4$, $b = 21.35$ mm, $T_o = 293.5$ K and $\theta_o = 29.35$ with the non-uniform grids. Because of the steep temperature gradient near the enclosure walls, the fine grids near the enclosure walls and the coarse grids in the core of the enclosure are performed with that the ratio of the width of the sequential grids is 1.2. The total average Nusselt number throughout the enclosure, \overline{Nu}_{total} , is

adopted to be a criterion test value. The criterion test values of the grid sizes 16×16, 20×20, 24×24, 28×28, 32×32 and 36×36 are calculated for the all schemes. The change of the criterion test values is less than 0.1% when the grid sizes are greater than or equal to 28×28 for the all schemes. Therefore, the grid size 28×28 is employed throughout this work.

4.1 Pure natural convection

The emissivity values of the wall surfaces of the square enclosure equal zero for the code validation with pure natural convection.

4.2 Natural convection with surface radiation

In this case, the code validation is carried out with that the emissivity values of the wall surfaces of the square enclosure are 0.5 and 1.0, and the conditions according to the solutions from the published numerical correlations and the published numerical solutions.

From the comparisons between the solutions of the in-house code with the benchmark numerical solutions, the solutions from the published numerical correlations and the published numerical solutions, most of the difference values are small, which they give the credence to the in-house code, while there are some difference values are great because of the existence of the errors of the correlations and the difference of the fluid properties used for the simulation.

TSF-1018

Table 1 Comparison between the solutions of the in-house code with the benchmark numerical solutions and the solutions from the published numerical correlations.

Ra	The solutions from the references \overline{Nu}_{conv}	Present study					
		\overline{Nu}_{conv}			Difference (%)		
		Central	Upwind	Hybrid	Central	Upwind	Hybrid
10^3	1.118 [1]	1.117	1.110	1.117	0.089	0.716	0.089
10^3	1.192 [3]	1.116	1.110	1.116	6.376	6.879	6.376
10^4	2.243 [1]	2.246	2.203	2.246	0.134	1.783	0.134
10^4	2.2415 [2]	2.246	2.203	2.246	0.201	1.718	0.201
10^4	2.408 [3]	2.246	2.203	2.246	6.728	8.513	6.728

Table 2 Comparison between the solutions of the in-house code with the solutions from the published numerical correlations and the published numerical solutions.

Ra	\mathcal{E}	The solutions from the references \overline{Nu}_{total}	Present study					
			\overline{Nu}_{total}			Difference (%)		
			Central	Upwind	Hybrid	Central	Upwind	Hybrid
10^3	0.5	1.579 [3]	1.642	1.637	1.642	3.990	3.673	3.990
10^3	0.1	2.125 [3]	2.271	2.266	2.271	6.871	6.635	6.871
10^4	0.5	3.264 [3]	3.225	3.179	3.225	1.195	2.604	1.195
10^4	0.5	4.078 [4]	3.617	3.569	3.616	11.305	12.482	11.329
10^4	1.0	4.470 [3]	4.510	4.461	4.510	0.895	0.201	0.895
10^4	1.0	5.260 [4]	5.410	5.360	5.409	2.852	1.901	2.833

Note for Table 1 and 2

1. The conditions of the solutions from the published numerical correlations [3] at $Ra = 10^3$ are $b = 7$ mm, $T_o = 298.15$ K and $\theta_o = 9.94$.
2. The conditions of the solutions from the published numerical correlations [3] at $Ra = 10^4$ are $b = 15$ mm, $T_o = 298.15$ K and $\theta_o = 9.94$.
3. The conditions of the published numerical solutions [4] are $b = 21.35$ mm, $T_o = 293.5$ K and $\theta_o = 29.35$.

5. Results and Discussion

Since the investigation is performed with a constant width of the enclosure, so that the temperature ratio has to vary with the Rayleigh number. The dimensions of the square enclosure

are imposed to be 21.35×21.35 mm. The variation of the temperature ratio with the Rayleigh number for present study at $T_o = 293.5$ K is shown in Fig. 3.

TSF-1018

Fig. 4 and 5 show the variation of the running time and the iteration numbers of the code with the Rayleigh number. From Fig. 4 and 5 at (a) and (c), the upwind differencing scheme took the least of time and the iteration numbers for running of the code. For the emissivity values of the enclosure surfaces equal 0.5, the upwind differencing scheme took the most of time for running of the code and the upwind differencing scheme took also the most of the iteration numbers for running of the code with the low values of the Rayleigh number while the central differencing scheme took the most of the iteration numbers for running of the code with the high values of the Rayleigh.

Fig. 6 and 7 show the velocity vectors and the dimensionless temperature contours in the square enclosure at $Ra = 10^4$, $T_o = 293.5$ K, $\theta_o = 29.35$ and $\mathcal{E} = 1.0$ with the various schemes.

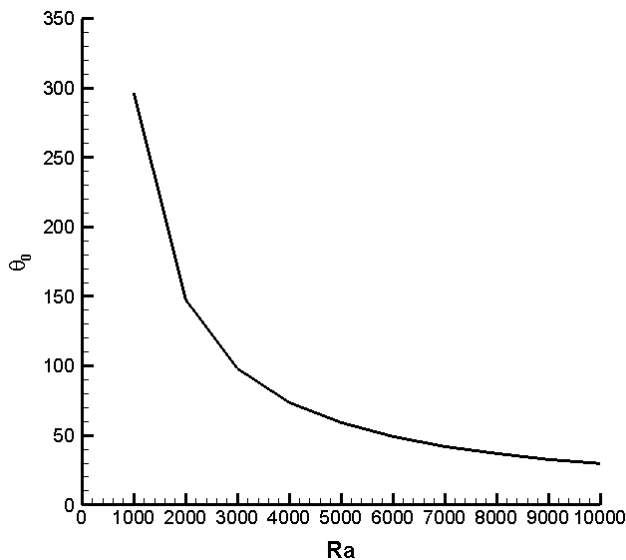


Fig. 3 Variation of the temperature ratio with the Rayleigh number for present study ($T_o = 293.5$ K).

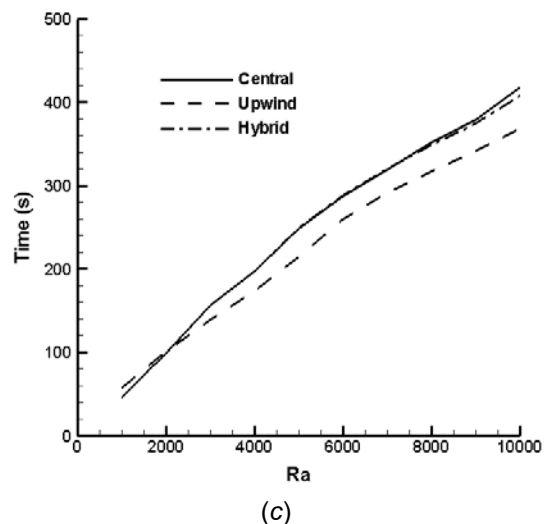
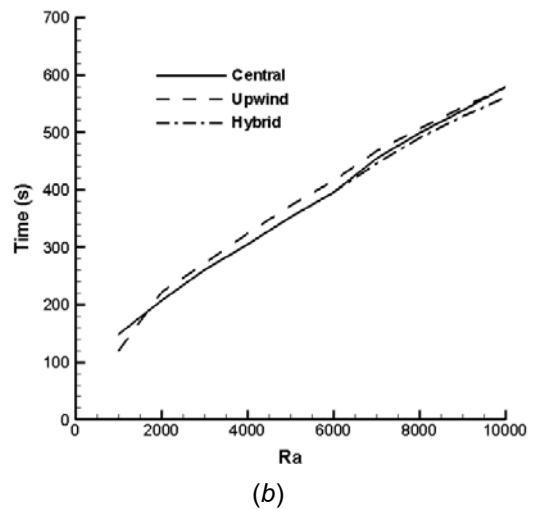
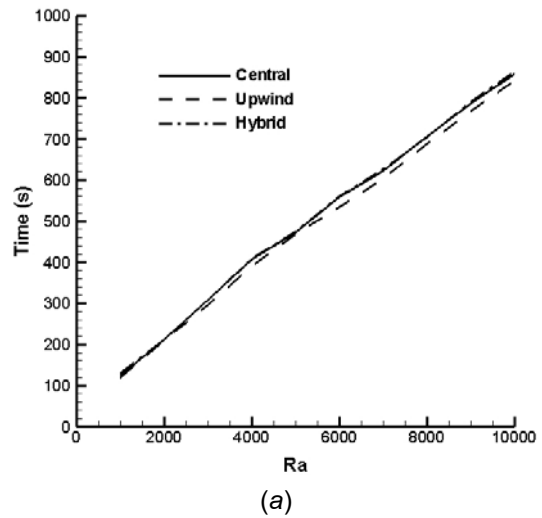
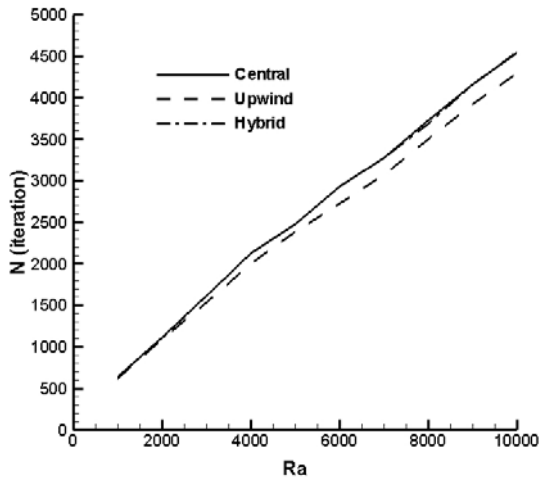
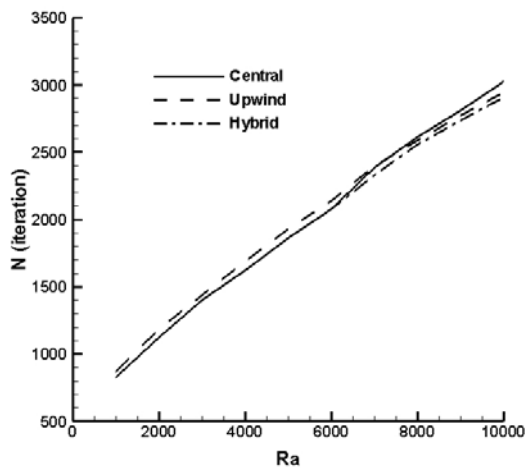


Fig. 4 Variation of the running time of the code with the Rayleigh number (a) $\mathcal{E} = 0.0$, (b) $\mathcal{E} = 0.5$, (c) $\mathcal{E} = 1.0$.

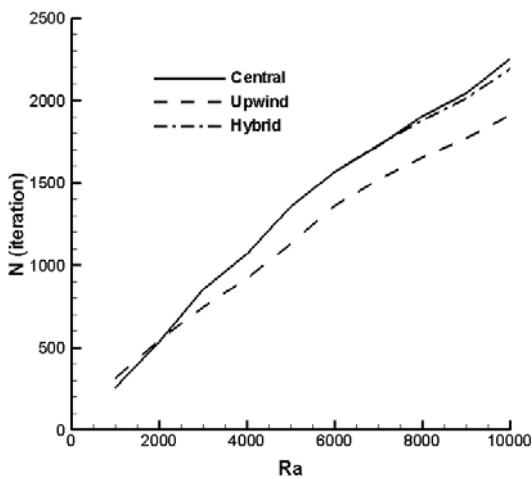
TSF-1018



(a)

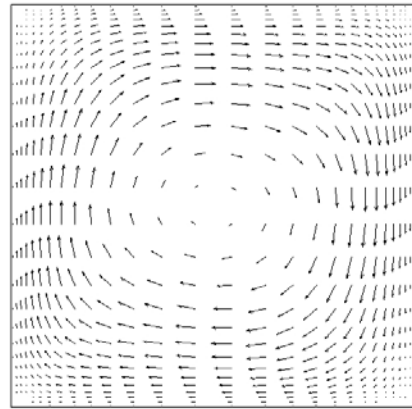


(b)

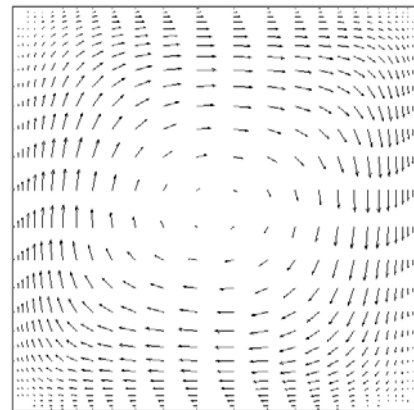


(c)

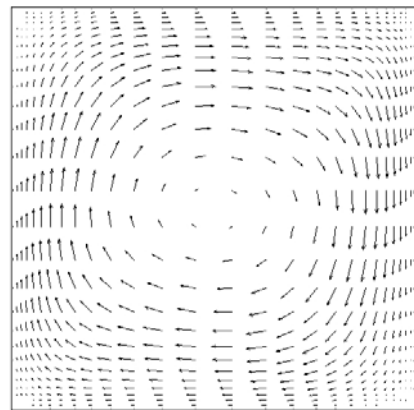
Fig. 5 Variation of the iteration numbers of the code with the Rayleigh number (a) $\mathcal{E} = 0.0$, (b) $\mathcal{E} = 0.5$, (c) $\mathcal{E} = 1.0$.



(a)



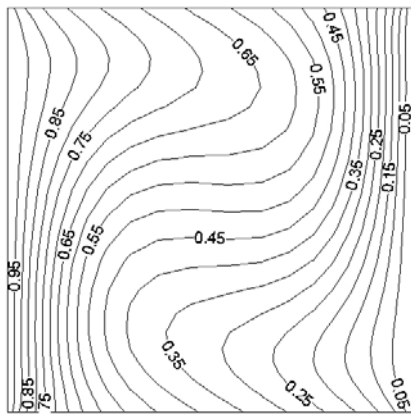
(b)



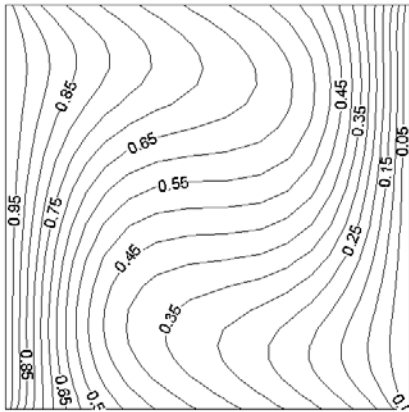
(c)

Fig. 6 Velocity vectors in the square enclosure ($Ra = 10^4$, $T_o = 293.5$ K, $\theta_o = 29.35$ and $\mathcal{E} = 1.0$) (a) Central differencing scheme, (b) Upwind differencing scheme, (c) Hybrid differencing scheme.

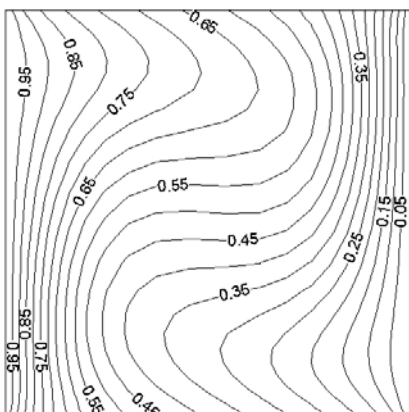
TSF-1018



(a)



(b)



(c)

Fig. 7 Dimensionless temperature contours in the square enclosure ($Ra = 10^4$, $T_0 = 293.5$ K, $\theta_0 = 29.35$ and $\mathcal{E} = 1.0$) (a) Central differencing scheme, (b) Upwind differencing scheme, (c) Hybrid differencing scheme.

6. Conclusion

For the emissivity values of the enclosure surfaces equal 0.0 and 1.0 the upwind differencing scheme can converge into the solutions more quickly than the other schemes.

7. Nomenclature

b	width of the enclosure
F	view factor
g	gravitational acceleration, ($= 9.81 \text{ m/s}^2$)
J	radiosity, W/m^2
k	thermal conductivity, $\text{W/(m}\cdot\text{K)}$
Nu	Nusselt number
P	pressure, Pa
q''	heat flux, W/m^2
Ra	Rayleigh number
T	temperature, K
T_0	reference temperature, K $\left(= \frac{T_H + T_C}{2} \right)$
T^*	dimensionless temperature $\left(= \frac{T - T_C}{T_H - T_C} \right)$
u	velocity component in the horizontal direction, m/s
v	velocity component in the vertical direction, m/s
V	total velocity, m/s
x	Cartesian coordinate in the horizontal direction of the enclosure, m
X^*	dimensionless coordinate in the horizontal direction of the enclosure $\left(= \frac{x}{b} \right)$
y	Cartesian coordinate in the vertical direction of the enclosure, m
Y^*	dimensionless coordinate in the vertical

direction of the enclosure $\left(= \frac{y}{b} \right)$

Greek symbols

ε emissivity

θ_0 Temperature ratio $\left(= \frac{T_0}{T_H - T_C} \right)$

μ viscosity, kg/s·m

ρ density, kg/m³

σ Stefan-Boltzmann constant,
(= 5.67051×10⁻⁸ W/(m²·K⁴))

Mathematical symbol

∇ del operator

Superscript

iter iteration number

Subscripts

ave average

A air

B bottom surface of the enclosure wall

conv convection

C cold wall

e eastern surface of cells

E eastern direction

H hot wall

i considered surface element

j the other surface element

n northern surface of cells

N northern direction

rad radiation

ref reference

s southern surface of cells

S southern direction

T top surface of the enclosure wall

w western surface of cells

W western direction

8. Acknowledgements

This research work is financially supported by Coordinating Center for Thai Government Science and Technology Scholarship Students (CSTS), National Science and Technology Development Agency (NSTDA), and Ministry of Science and Technology (MOST) under the project "A New Researcher Scholarship of CSTS, MOST", the contract No. 31/2554, and the project code SCH-NR2011-252. This support is gratefully acknowledged.

Appreciation is extended to the Faculty of Engineering, Burapha University for the facility support.

9. References

- [1] G. De Vahl Davis (1983). Natural convection of air in a square cavity a bench mark numerical solution, *International Journal for Numerical Methods in Fluids*, vol. 3, pp. 249-264.
- [2] T. Saitoh and K. Hirose (1989). High-accuracy bench mark solutions to natural convection in a square cavity, *Computational Mechanics*, vol. 4, pp. 417-427.
- [3] C. Balaji and S. P. Venkateshan (1994). Correlations for free convection and surface radiation in a square cavity, *International Journal of Heat and Fluid Flow*, vol. 15, pp. 249-251.
- [4] M. Akiyama and Q. P. Chong (1997). Numerical analysis of natural convection with surface radiation in a square enclosure, *Numerical Heat Transfer, Part A*, vol. 31, pp. 419-433.

TSF-1018

[5] Nilesh Agrawal, Seik Mansoor Ali, K. Velusamy and Sarit K. Das (2012). A correlation for heat transfer during laminar natural convection in an enclosure containing uniform mixture of air and hydrogen, International Communications in Heat and Mass Transfer, vol. 39, pp. 24-29.

[6] Mostafa Mahmoodi (2011). Numerical simulation of free convection of nanafluid in a square cavity with an inside heater, International Journal of Thermal Sciences, vol. 50, pp. 2161-2175.

[7] J. Xaman, J. Arce, G. Alvarez and Y. Chavez (2008). Laminar and turbulent natural convection combined with surface thermal radiation in a square cavity with a glass wall, International Journal of Thermal Sciences, vol. 47, pp. 1630-1638.

[8] H. K. Versteeg and W. Malasekera (2007). An Introduction to Computational Fluid Dynamics the Finite Volume Method, 2nd edition., Pearson Education Limited.